Water Environment Federation
the water quality people

Turbulence and interphase mass diffusion assumptions on the performance of secondary settling tanks

Haiwen Gao, Michael K. Stenstrom*

Department of Civil and Environmental Engineering, University of California, Los Angeles, Los Angeles, California

Received 2 April 2018; Revised 22 May 2018; Accepted 21 June 2018

Correspondence to: Michael K. Stenstrom, Department of Civil and Environmental Engineering, University of California, Los Angeles, Los Angeles, CA.
Email: stenstro@seas.ucla.edu

*WEF Member

Published online 18 January 2019 in Wiley Online Library (wileyonlinelibrary.com)

DOI: 10.1002/wer.1003

Abstract

Secondary settling tanks (SSTs), also known as secondary sedimentation tanks or secondary clarifiers, are a basic yet complicated process in a biological water resource recovery facility. In order to understand and improve SST performance, computational fluid dynamics methods have been employed over the last 30 years. In the present investigation, a Fluent-based two-dimensional axisymmetric numerical model is applied to understand the effects of the buoyancy term (G_b) in the turbulent kinetic energy (TKE) equation and two model parameters (the coefficient of buoyancy term (C_3) in the turbulent dissipation rate equation and the turbulent Schmidt number (σ_c) in the sludge transport equation) on the performance of an SST. The results show that the hydrodynamics can only be correctly predicted by buoyancy-coupled TKE equation, unless the mixed liquor suspended solids is low and sludge settling velocity is extremely high. When the field observations show the SST is operating well, the buoyancy-decoupled TKE equation predicts the correct result, but the buoyancy-decoupled TKE equation may predict failure. Care is required in selecting the correct modeling technique for various conditions. This study provides guidance on how to avoid modeling problems and increase rates of convergence. © 2018 Water Environment Federation

Practitioner points

- C3 can be set to zero to improve rate of convergence and reduce computing time.
- σc can be used to adjust SBH, when ESS and RAS concentrations are well calibrated to the field data, but the SBH does not fit field observation.

Key words

buoyancy effects; computational fluid dynamics modeling; Realizable *k*-ε model; secondary settling tank; turbulent Schmidt number

Introduction

In conventional water resource recovery facilities, bioreactors with aeration (Hwang & Stenstrom, 1985) are connected to secondary settling tanks (SSTs) to remove organic matter and reduce nutrients such as nitrogen and phosphorus by gravity sedimentation (Ramin et al., 2014). Secondary settling tanks (SSTs), also known as sedimentation tanks or secondary clarifiers, have two different functions: clarification and thickening (Parker, 1983). Clarification is used to separate the suspended biomass from the effluent. Thickening is used to concentrate the sludge in order to recycle or dispose of it in less volume (Gao & Stenstrom, 2017). In SSTs, the clarification process happens in the upper layer, whereas thickening occurs near the bottom. This results in an effluent with a low concentration of suspended solids flowing out from the top and a second stream, with highly concentrated sludge, from the bottom (Li & Stenstrom, 2014).

Previously, design procedures for SSTs were more empirical, which were based on hydraulic criteria such as surface overflow rate (SOR) and hydraulic retention time (HRT; Coe & Clevenger, 1916). Without understanding the internal flow field and solids distribution, SSTs' performance can suffer unanticipated fluctuations, which may reduce performance and increase the risks of failure. Therefore, computational fluid dynamics (CFD) models of SSTs have been developed to illuminate the "black box" and to understand the different influential processes in the SSTs (Imam, McCorquodale, & Bewtra, 1983; Larsen, 1977; Zhou & McCorquodale, 1992b).

As flow in SSTs is driven by density, experiments have been performed to understand the nature of the flow in SSTs, and different mathematical models have been proposed to describe this phenomenon (DeVantier & Larock, 1986, 1987; Lakehal, Krebs, Krijgsman, & Rodi, 1999; Lyn, Stamou, & Rodi, 1992; Stamou, Adams, & Rodi, 1989; Zhou & McCorquodale, 1992a, 1992c). Larsen (1977) was the pioneer in the CFD study of SSTs and sets the framework of the CFD study for the future SST research. Since then, research has mostly focused on (a) improving the prediction accuracy of the CFD models by understanding the hydrodynamics of the SSTs (Adams & Rodi, 1990; Lakehal et al., 1999; Lyn et al., 1992; Zhou & McCorquodale, 1992b); and (b) optimizing the operation (e.g., inflow rate, inlet mixed liquor suspended solids (MLSS), returned activated sludge (RAS) ratio) and internal geometry of the SSTs (Deininger, Günthert, & Wilderer, 1996; Griborio, 2004; Krebs, Vischer, & Gujer, 1995; Patziger, 2016; Vitasovic, Zhou, McCorquodale, & Lingren, 1997; Zhou & McCorquodale, 1992a).

DeVantier and Larock (1986) were the first researchers to study the effects of buoyancy term (G_b) in the standard k-ε turbulence model (SKE). However, because of the strong local numerical instabilities along the reaction baffle, the flow in the inlet zone was not modeled and the opening under the bottom baffle lip was chosen as the inlet boundary. Additionally, as the result of a coarse mesh caused by limited computational storage, the SKE model was locally divergent. Also, as a result of convergence difficulty for the flow with high MLSS concentration, the modeled inlet solids concentration was very low (only 750 mg/L). In the follow-on study, DeVantier and Larock (1987) overcame these difficulties by decoupling the buoyancy term. This improved the simulation results but ignored buoyancy effects on the turbulence model.

Zhou and McCorquodale (1992a,b) also ignored the buoyancy term in the turbulence model when analyzing the hydrodynamics of SSTs. However, the modeled inlet concentration of MLSS in their studies was low (only 1,400 mg/L). Hence, their simulation results may be limited to SSTs operating with low inlet solids concentrations.

Vitasovic et al. (1997) applied a two-dimensional model to study the effects of surface overflow rate (SOR) and to optimize the internal structure of the SST. The buoyancy term was also ignored in their turbulence model. Some of their predictions were opposite to the simulation results predicted by the Quasi-3D (Q3D) model in Gao and Stenstrom (2017).

The latest CFD SST model decoupling the buoyancy term in a turbulence model was in Tamayol, Firoozabadi, and Ashjari (2009). In this study, the effects of Froude and Reynolds numbers on the flow field and optimal baffle location were studied. However, no calibration procedure of their model was reported; therefore, the reliability of their model results is doubtful.

More recent studies, essentially after the 1990s, have included the buoyancy term in their models, and many have compared their simulation results with field data (Dahl, 1993; Lakehal et al., 1999; Lyn et al., 1992; Ramin et al., 2014; Shahrokhi, Rostami, Said, Yazdi, & Syafalni, 2013; Xanthos et al., 2010). However, none have compared simulation results with and without coupling the buoyancy term. Therefore, none of the previous studies have confirmed the need to couple the buoyancy term in a turbulence model. Also, the buoyancy coefficient (C_3) applied in the turbulent dissipation rate (TDR) equation varied widely among the studies. Interpreting the results are further complicated using a wide range of the turbulent Schmidt numbers (σ_c). Table 1 shows the wide range of buoyancy coefficients and turbulent Schmidt numbers used previously.

In the present work, sensitivity tests using the Realizable k-ε model are performed to understand (a) the necessity of coupling the buoyancy term in a turbulence kinetic energy (TKE) equation; and (b) the effects of two model parameters (the coefficient of buoyancy term (C_3) in the TDR equation and the turbulent Schmidt number (σ_c) in the sludge transport equation). Firstly, simulation results are presented by coupling and decoupling the buoyancy term in the TKE equation and then comparing the two results. Next, the effects of inlet MLSS concentration and sludge settling properties are illustrated without coupling the buoyancy term in the TKE equation. Finally, the effects of varying the C_3 and the σ_c on the hydrodynamics of SST are compared.

Methodology

The numerical model

Figure 1 shows the geometry and the boundary conditions of the model. As the current research focuses on the parameters

Table 1. Applications of the two model parameters: (a) coefficient of the buoyancy term (C_3) in the TDR equation; and (b) turbulent Schmidt number in the sludge transport model from the literature

TURBULENT SCHMIDT NUMBER		
Σ_Y	Σ_R	REFERENCES
0.5	0.5	Stamou et al. (1989)
0.7	0.7	
1.0	1.0	
1.0	0.5	Zhou and McCorquodale (1992a)
1.0	1.0	Zhou and McCorquodale (1992c)
0.5	1.0	
1.0	1.0	Dahl (1993)
0.7	0.7	Lakehal et al. (1999)
0.5–0.9	0.7	Saffarian et al. (2010)
1.0	1.0	Ramin et al. (2014)
Coefficient of Buoyancy term (C_3)		
0.15		Ramin et al. (2014)
0.2		Dahl (1993), Shahrokhi et al. (2013)
0–0.2		Lakehal et al. (1999), Saffarian et al. (2010)
0.8		Xanthos et al. (2010)

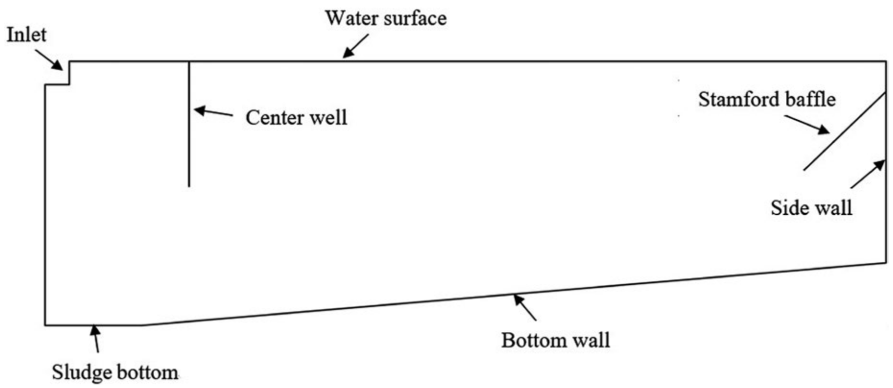

Figure 1. Geometry and boundary conditions of the circular SST.

in the turbulence model and the sludge transport model, only these two models are shown below. A more detailed description of CFD model non-Newtonian flow behavior of the activated sludge and buoyancy effects is shown in Gao and Stenstrom (2018).

The Realizable k-ε model is:

$$\frac{\partial k}{\partial t}+u\frac{\partial k}{\partial r}+v\frac{\partial k}{\partial y}=\frac{\partial}{\partial r}\left[\left(\vartheta+\frac{\vartheta_t}{\sigma_k}\right)\frac{\partial k}{\partial r}\right]+\frac{\partial}{\partial y}\left[\left(\vartheta+\frac{\vartheta_t}{\sigma_k}\right)\frac{\partial k}{\partial y}\right] +G_k+G_b-\rho\varepsilon, \quad (1)$$

and:

$$\frac{\partial \varepsilon}{\partial t}+u\frac{\partial \varepsilon}{\partial r}+v\frac{\partial \varepsilon}{\partial y}=\frac{\partial}{\partial r}\left[\left(\vartheta+\frac{\vartheta_t}{\sigma_\varepsilon}\right)\frac{\partial \varepsilon}{\partial r}\right]+\frac{\partial}{\partial y}\left[\left(\vartheta+\frac{\vartheta_t}{\sigma_\varepsilon}\right)\frac{\partial \varepsilon}{\partial y}\right] -C_1\frac{\varepsilon}{k}C_3G_b+\rho C_1S\varepsilon-\rho C_2\frac{\varepsilon^2}{k+\sqrt{\vartheta\varepsilon}}. \quad (2)$$

G_k represents the generation of TKE as a result of the mean velocity gradients, and G_b corresponds to the generation of TKE as a result of buoyancy.

$$G_k=\vartheta_t\left[2\left(\frac{\partial u}{\partial r}\right)^2+2\left(\frac{\partial v}{\partial y}\right)^2+2\left(\frac{u}{r}\right)^2+\left(\frac{\partial u}{\partial y}+\frac{\partial v}{\partial r}\right)^2\right] \quad (3)$$

$$G_b=-g\frac{\vartheta_t}{\sigma_t}\frac{\partial \rho}{\partial y}, \quad (4)$$

$$C_1=\max\left[0.43,\frac{\eta}{\eta+5}\right],\eta=\frac{Sk}{\varepsilon}. \quad (5)$$

The turbulent viscosity, ϑ_t, is then determined as a function of TKE (k) and its TDR (ε) by:

$$\vartheta_t=C_\mu\frac{k^2}{\varepsilon}. \quad (6)$$

However, C_μ is no longer constant and is a function of the mean strain and rotation rates, the angular velocity of the system rotation, and the turbulent fields. The sludge transport model is:

$$u\frac{\partial C}{\partial r}+v\frac{\partial C}{\partial y}=\frac{1}{r}\frac{\partial}{\partial r}\left[r\left(\vartheta+\frac{\vartheta_t}{\sigma_r}\right)\frac{\partial C}{\partial r}\right] +\frac{1}{r}\frac{\partial}{\partial y}\left[r\left(\vartheta+\frac{\vartheta_t}{\sigma_y}\right)\frac{\partial C}{\partial y}-rV_sC\right] \quad (7)$$

in which C is the sludge concentration,ϑ is the viscosity of the sludge mixture, ϑ_t is the turbulent eddy viscosity, and σ_r and σ_y are the turbulent Schmidt numbers in the r and y directions, respectively. V_s is the particle settling velocity determined by the Takács equation (Takács, Patry, & Nolasco, 1991) or other equations (Saffarian, Hamedi, & Shams, 2010).

Boundary conditions

The velocity inlet boundary condition is applied to the inlet and sludge bottom boundaries. A pressure outlet boundary condition is applied for the surface outlet boundary, which assumes a uniform pressure and zero-gradient for all transport variables. For the free ambient water surface, the rigid-lid approximation for all velocity components with full slip shear condition is assumed. The free surface boundary is treated as a symmetry condition. The solid boundaries are specified as stationary walls with no shear.

Model verification

The simulation results are compared with the field data from Griborio (2004) and shown in another paper (Gao & Stenstrom, 2018). ESS and RAS concentration are fitting parameters.

Results and Discussion

The effects of buoyancy term G_b in the TKE equation

Effects on performance indicators. In Griborio's dissertation, four Darvill SST test cases (Tests 1–4) from Ekama and Marais (2002) were compared. The loading conditions for these four tests are shown in Table 2. The field observations of the ESS and SBH for Test 4 are not available, but the field observations of the ESS and SBH for Tests 1–3 are available and therefore compared with the predictions of the buoyancy-decoupled/coupled turbulence models. The comparisons are shown in Table 3. Additionally, the predictions of the ESS for Tests 1–3 by the SettlerCAD model and the two-dimensional model (2Dc; Griborio, 2004) are also included in Table 3. The SettlerCAD model was developed based on the CFD model of Zhou and McCorquodale (1992b). This model uses an SKE model without coupling the buoyancy terms. The 2Dc model was developed at the University of New Orleans. The turbulence model is based on mixing length theory. Comparisons for Tests

Table 2. Loading conditions for the three test cases on the Darvill SST

LOADING CONDITIONS[a]	TEST 1	TEST 2	TEST 3
Averaged SOR (m/hr)	0.866	0.715	0.985
Averaged $Q_{effluent}$ (m^3/hr)	833	688	948
Recycle ratio	0.80	0.97	0.79
Averaged MLSS (mg/L)	4,600	4,300	3,600

Note. [a]Values were reported by Ekama and Marais (2002) and used by Griborio (2004).

1–3 are based on a "safe/fail" basis. SST failure is defined as an ESS greater than 30 mg/L or the sludge blanket rising to the SST surface.

Table 3 shows that the buoyancy-coupled turbulence model not only correctly predicts the safe operation for all three tests, but also predicts similar ESS to the field observations for all three tests. However, the not only buoyancy-decoupled turbulence model predicts the failure for all three tests, but the predicted ESS are significantly different from the field observations. The SettlerCAD model also predicts the failure for Tests 1 and 2 because of high ESS, and the predictions are remarkably different from the field observations. The results of the buoyancy-decoupled/coupled turbulence models in this study and the results of the SettlerCAD model show that coupling/decoupling the buoyancy term in the TKE equation has significant influence in predicting the SST performance. The application of the buoyancy-coupled turbulence model is more reliable.

Table 3. Comparison among the results of the actual stress tests, the prediction results of the SettlerCAD model, and the prediction results of the G_b-decoupled/G_b-coupled turbulence models

	TEST 1	TEST 2	TEST 3
Actual stress tests[a]			
SBH[b] (m)	2.20	2.60	2.70
ESS (mg/L)	17	5	10
SettlerCAD results[a]			
ESS (mg/L)	495	933	2.1
Test outcome[c]	Fail	Fail	Safe
2Dc results[d]			
ESS (mg/L)	17	5.0	10
Test outcome[c]	Safe	Safe	Safe
Fluent model[e]			
SBH[b] (m):	0	0	0
G_b-decoupled/G_b-coupled	3.2	3.0	3.2
ESS (mg/L):	2,650	2,792	1,550
G_b-decoupled/G_b-coupled	8	8	10
Test outcome[c] for the G_b-decoupled	Fail	Fail	Fail
Test outcome[c] for the G_b-coupled	Safe	Safe	Safe

Notes. [a]Values were reported by Ekama and Marais (2002) and used by Griborio (2004).
[b]SBH is the depth between the water surface and the sludge blanket surface.
[c]SST failure is defined as the ESS ≥ 30 mg/L or the sludge blanket rising to the SST surface.
[d]Values were reported by Griborio (2004).
[e]G_b-decoupled and G_b-coupled turbulence models are applied in this study's simulations.

Effects on turbulent viscosity. Figure 2a,b compares the distributions of turbulent viscosity (ϑ_t) with buoyancy-decoupled/coupled TKE equations when the inflow rate (Q) is 1,500 m^3/hr, MLSS is 4,600 mg/L, and the RAS ratio is 0.8. Without coupling the buoyancy term in the TKE equation (Figure 2a), the highly turbulent viscosity is extended from the inlet zone to the entire main settling zone, and from the surface of the SST to the bottom sludge outlet. However, coupling the buoyancy term in the TKE equation (Figure 2b) reduces the highly turbulent viscosity and is only presented inside the inlet zone. Outside the inlet zone, the turbulent viscosity (turbulent mixing) is globally reduced as a result of density stratification in the SST. A decrease inϑ_t, in turn, causes a decrease of the turbulent diffusive transport of all quantities (Lakehal et al., 1999).

Effects on settling velocity. Figure 3a,b shows the settling velocity profiles with buoyancy-coupled/decoupled in the TKE equation (Q = 1,500 m^3/hr, MLSS = 4,600 mg/L, RAS ratio = 0.8). Without coupling the buoyancy term in the TKE equation, the distribution of large turbulent viscosity is present over the entire SST, as shown in Figure 2a, and causes poor particle settling (Figure 3a), even with good particle settling properties. Maximum settling velocity occurs at the surface of the SST but is much lower than the maximum settling velocity in the coupled result, which occurs at the surface of the sludge blanket.

Effects on sludge concentration. Figure 4a,b shows the sludge concentration profiles by a buoyancy-coupled and buoyancy-decoupled TKE equation (Q = 1,500 m^3/hr, MLSS = 4,600 mg/L, RAS ratio = 0.8). Without the buoyancy term coupled in TKE equation (Figure 4b), the sludge does not settle well and is stratified vertically and well-mixed horizontally throughout the radius of the SST. This is opposite to Lyn's results (Lyn et al., 1992), which showed very little vertical stratification. However, with the buoyancy term coupled in the TKE equation, turbulent mixing is globally damped and the sludge blanket exhibits a distinct interface at the upper clarification zone and bottom thickening zone (Figure 4a).

The effects of sludge concentration and settling velocity with buoyancy-decoupled/coupled TKE equation

To confirm whether the buoyancy term in the TKE equation can be neglected when the MLSS concentration is low, or the settling velocity is significantly large, coupled and decoupled simulations are performed with four gradually decreasing MLSS concentrations and five gradually increasing settling velocities (Q = 1,500 m^3/hr, RAS ratio = 0.8). All the predicted ESS concentrations are summarized in Figure 5a,b. As Zhou and McCorquodale (1994) showed, the usual range of settling velocity (V_s) in SSTs is from 7.0 to 11.0 m/hr, which means the Stokes velocity constant (V_o) in the Takács equation (Takács et al., 1991) is from 8.0 to 13.0 m/hr. These values correspond to the current sludge empirical coefficients for rapid and slow settling (r_p = 0.39 L/g; r_h = 10 L/g; Griborio, 2004). Sensitivity

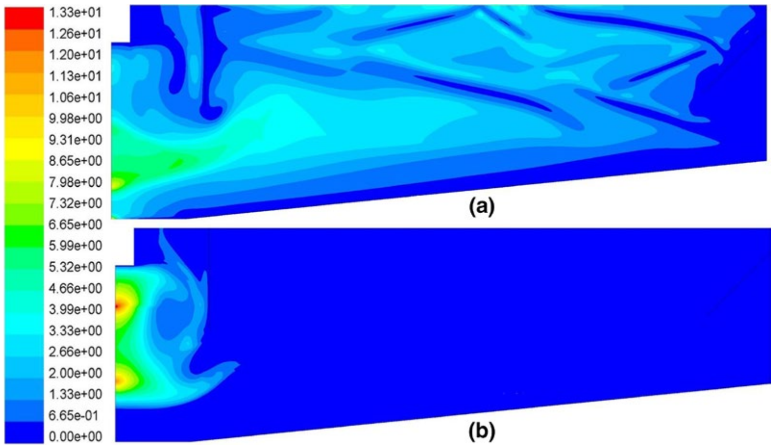

Figure 2. Distribution of turbulent viscosity (kg m^{-1} s^{-1}): (a) buoyancy-decoupled; (b) buoyancy-coupled TKE equation (Q = 1,500 m^3/hr, MLSS = 4,600 mg/L, RAS ratio = 0.8).

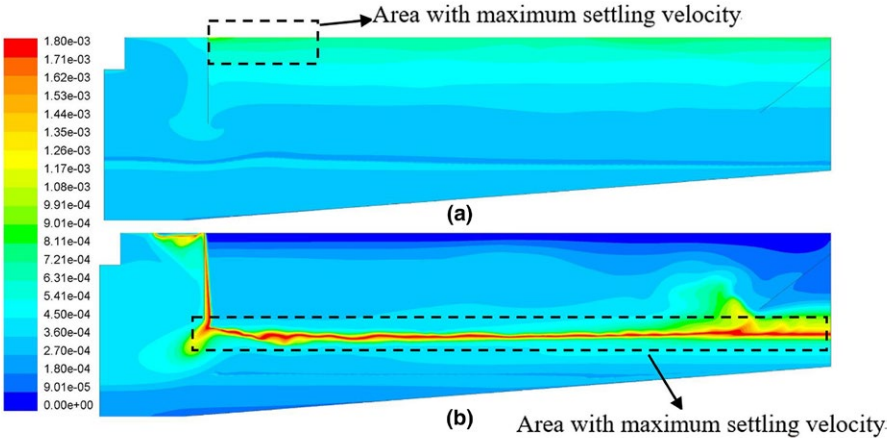

Figure 3. Distribution of sludge settling velocity (m/s): (a) buoyancy-decoupled; (b) buoyancy-coupled TKE equation (Q = 1,500 m^3/hr, MLSS = 4,600 mg/L, RAS ratio = 0.8).

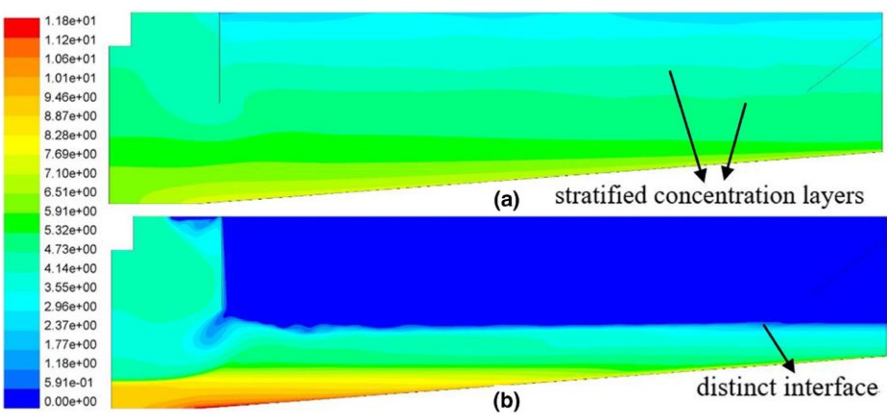

Figure 4. Distribution of sludge concentration (g/L): (a) buoyancy-decoupled; (b) buoyancy-coupled TKE equation (Q = 1,500 m^3/hr, MLSS = 4,600 mg/L, RAS ratio = 0.8).

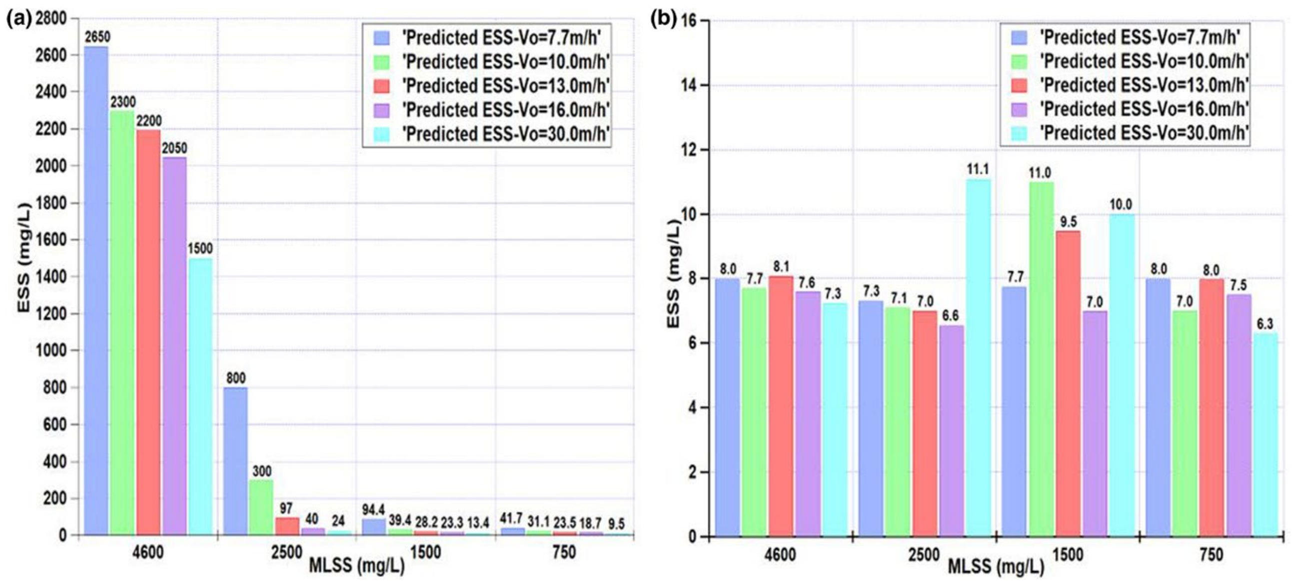

Figure 5. Predicted ESS with four different MLSS concentrations and five Stokes velocities V_o: (a) buoyancy-decoupled; (b) buoyancy-coupled (Q = 1,500 m^3/hr, RAS ratio = 0.8).

tests of sludge settling velocity on ESS start from V_o = 7.7 m/hr (the original Stokes velocity) and extend to an extremely high V_o (30 m/hr), the maximum velocity reported in previous research (Zhou & McCorquodale, 1992b).

In the original case (MLSS = 4,600 mg/L), the buoyancy-coupled TKE equation (Figure 5a) predicts an ESS concentration similar to the field observations (7–8 mg/L simulated compared to 17 mg/L observed). In the buoyancy-decoupled TKE equation (Figure 5b), there is a large divergence between field observations and simulation results; the simulation shows failure of the SST. With a decrease in MLSS concentration or an increase in sludge settling velocity, the ESS predicted by the buoyancy-coupled TKE equation shows a negligible change of ESS concentration and all the simulations show the SST is operating well, compared to excessive ESS predicted by the buoyancy-decoupled TKE equation. The predicted ESS at 4,600 mg/L MLSS concentration averaged over the five settling velocities is approximately 7–8 mg/L. Figure 5b shows excessive ESS at 4,600 mg/L MLSS which decreases with increasing settling velocity but remains excessive. The ESS decreases with decreasing MLSS concentration under the same sludge settling velocity, but also remain excessive.

The buoyancy-coupled TKE equation predicts reasonable ESS for all MLSS concentrations and settling velocities. The decoupled TKE equation rarely predicts reasonable ESS, and then only for MLSS concentrations of 1,500 mg/L or less, with settling velocities of 13 m/hr or greater. All predictions of ESS by the buoyancy-coupled TKE equation (Figure 5a) are reasonable, whereas the predictions of ESS by the buoyancy-decoupled TKE equation show the failure of SST even with an extremely high settling velocity. The buoyancy-decoupled TKE predicts plausible results only when MLSS is below 1,500 mg/L, with settling velocities of 13 m/hr or greater. The buoyancy-decoupled TKE equation is of limited value, being useful only at low MLSS concentrations with high settling velocities. This is a severe limitation as SST operating with low MLSS and well-settling sludge rarely fail, and there is less incentive to model them. Cases with high MLSS and poorer settling are more likely candidates for modeling.

The effects of the coefficient (C_3) of the buoyancy term in the TDR equation

Lakehal et al. (1999) showed that the SBH, the magnitude and the location of the peak horizontal velocity, and the peak gradients of both horizontal and concentration are sensitive to the value of C_3, but did not show the effects of C_3 on performance indicators, such as ESS and RAS concentrations. To understand the potential effect of C_3 on ESS and RAS concentrations, a sensitivity study is conducted by varying C_3 using two flow rates. The results are shown in Table 4.

At the original inflow rate (Q = 1,500 m^3/hr, MLSS = 4,600 mg/L, RAS ratio = 0.8), the simulation predicts that increasing C_3 causes a gradual decrease in all the turbulent quantities. This occurs because increasing C_3 in the TDR equation causes an increase in TDR. The increase in TDR, in turn, causes a decrease in the turbulent eddy viscosity ϑ_t, decreasing the turbulent diffusive transport parameters, consistent with the results of Lakehal et al. (1999).

The effects of decreased turbulent diffusion can also be demonstrated by comparing the velocity contours in Figure 6a,b and the concentration contours in Figure 7a,b. Each contour in these two figures shows the profile predicted with $C_3 = 0$ and $C_3 = 1$, respectively. In Figure 6a,b, as the eddy diffusion is more intense with $C_3 = 0$, a series of small eddies along the horizontal jet is generated (highlighted in six black rectangular boxes in Figure 6a). As C_3 increases, the small eddies gradually

Table 4. Effects of the coefficient of buoyancy term (C_3) on different performance indicators at the original inflow rate (Q) and 20% increase of inflow rate (1.2Q)

	TURBULENT INTENSITY (%)		TKE (M^2/S^2)		TURBULENT VISCOSITY (KG M^{-1} S^{-1})		ESS (MG/L)		RAS (MG/L)		SBH (M)	
C_3	Q	1.2Q	Q	1.2Q	Q	1.2Q	Q	1.2Q	Q	1.2Q	Q	1.2Q
0	3.02	2.82	1.36	1.20	15.0	2.70	8.2	12.0	10,400	10,200	3.2	2.7
0.2	2.96	2.84	1.31	1.21	15.0	3.31	8.0	10.7	10,300	10,100	3.2	2.7
0.4	2.91	2.91	1.27	1.27	11.9	5.33	10.5	11.0	10,200	10,000	3.2	2.8
0.6	2.74	2.82	1.13	1.19	10.5	3.59	10.0	9.5	10,100	10,300	3.2	2.5
0.8	2.70	2.81	1.10	1.19	10.1	5.31	9.5	8.5	10,000	10,200	3.2	2.5
1.0	2.66	2.82	1.01	1.19	9.7	9.10	12.3	10.6	10,000	10,300	3.2	2.5

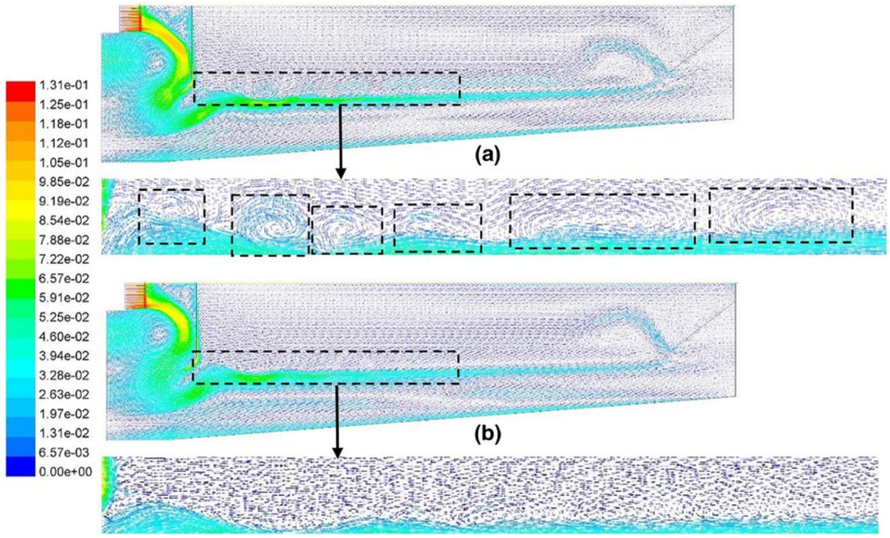

Figure 6. Effects of the coefficient of buoyancy term (C_3) on velocity distribution (m/s) with the original inflow rate (Q = 1,500 m^3/hr, MLSS = 4,600 mg/L, RAS ratio = 0.8): (a) C_3 = 0, presence of a series of eddies along the horizontal jet; (b) C_3 = 1.0, absence of eddies along the horizontal jet.

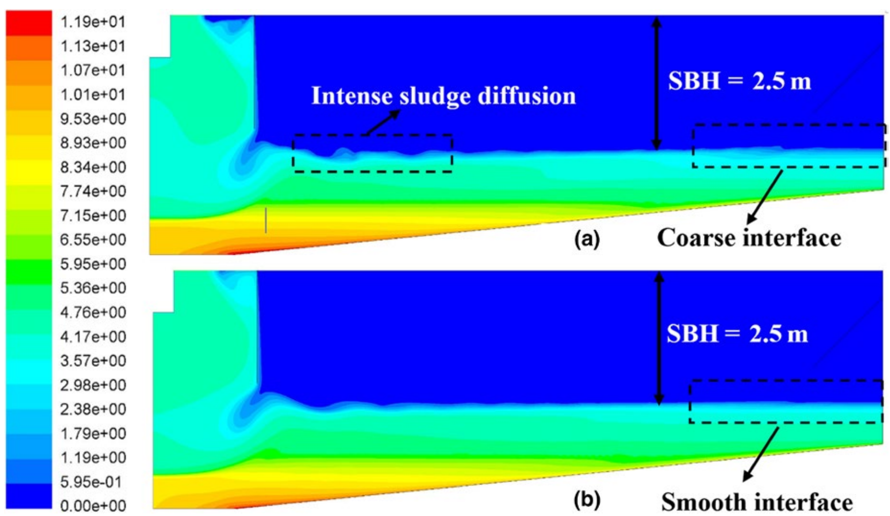

Figure 7. Effects of the coefficient of buoyancy term (C_3) on sludge concentration (g/L) with the original inflow rate (Q = 1,500 m^3/hr, MLSS = 4,600 mg/L, RAS ratio = 0.8): (a) C_3 = 0; (b) C_3 = 1.0.

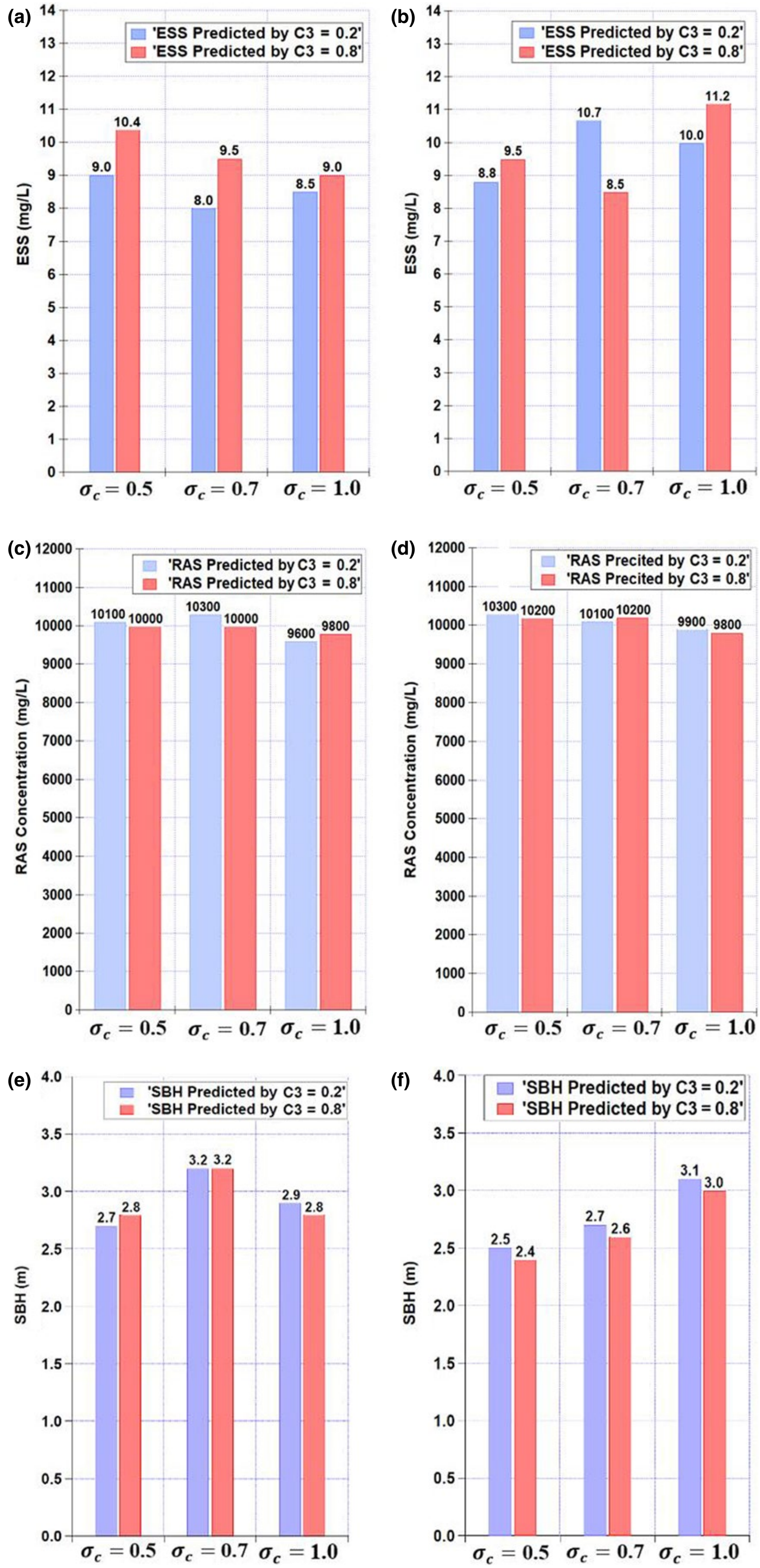
(a)
'ESS Predicted by C3 = 0.2'
'ESS Predicted by C3 = 0.8'
ESS (mg/L)
9.0
10.4
8.0
9.5
8.5
9.0
$\sigma_c = 0.5$
$\sigma_c = 0.7$
$\sigma_c = 1.0$
(b)
'ESS Predicted by C3 = 0.2'
'ESS Predicted by C3 = 0.8'
ESS (mg/L)
8.8
9.5
10.7
8.5
10.0
11.2
$\sigma_c = 0.5$
$\sigma_c = 0.7$
$\sigma_c = 1.0$
(c)
'RAS Predicted by C3 = 0.2'
'RAS Predicted by C3 = 0.8'
RAS Concentration (mg/L)
10100
10000
10300
10000
9600
9800
$\sigma_c = 0.5$
$\sigma_c = 0.7$
$\sigma_c = 1.0$
(d)
'RAS Precited by C3 = 0.2'
'RAS Precited by C3 = 0.8'
RAS Concentration (mg/L)
10300
10200
10100
10200
9900
9800
$\sigma_c = 0.5$
$\sigma_c = 0.7$
$\sigma_c = 1.0$
(e)
'SBH Predicted by C3 = 0.2'
'SBH Predicted by C3 = 0.8'
SBH (m)
2.7
2.8
3.2
3.2
2.9
2.8
$\sigma_c = 0.5$
$\sigma_c = 0.7$
$\sigma_c = 1.0$
(f)
'SBH Predicted by C3 = 0.2'
'SBH Predicted by C3 = 0.8'
SBH (m)
2.5
2.4
2.7
2.6
3.1
3.0
$\sigma_c = 0.5$
$\sigma_c = 0.7$
$\sigma_c = 1.0$

Figure 8. Effects of turbulent Schmidt number on the prediction of ESS, RAS concentration, and SBH at different inflow rates and different C_3: (a) ESS—original inflow rate (Q); (b) ESS—20% increment of inflow rate (1.2Q); (c) RAS concentration—Q; (d) RAS concentration—1.2Q; (e) SBH-Q; (f) SBH-1.2Q (Q = 1,500 m^3/hr, 1.2Q = 1,800 m^3/hr, MLSS = 4,600 mg/L, RAS ratio = 0.8).

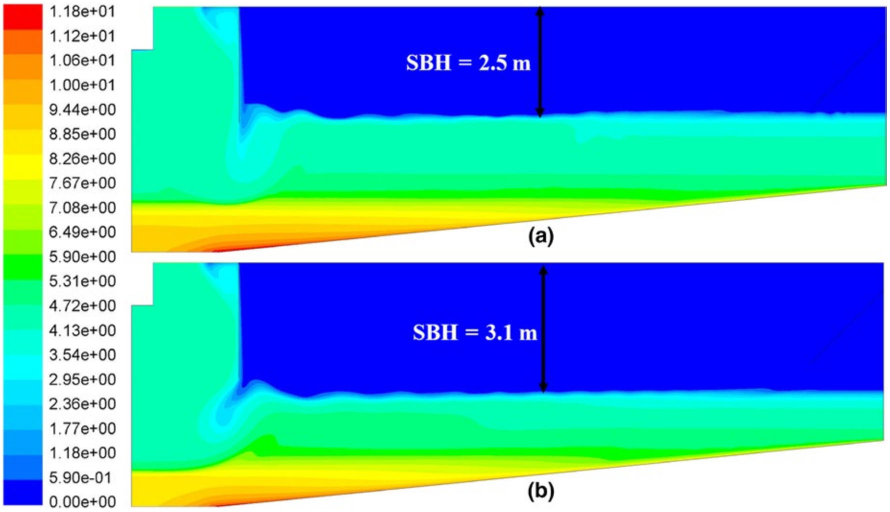

Figure 9. Effects of the turbulent Schmidt number on sludge concentration (g/L) at 20% increment of inflow rate (1.2Q = 1,800 m^3/hr, MLSS = 4,600 mg/L, RAS ratio = 0.8): (a) σ_c = 0.5; (b) σ_c = 1.0.

decline and finally disappear. Therefore, the sludge blanket exhibits a smoother concentration gradient at the interface, as shown in Figure 7b.

However, in contrast with the simulation results in Lakehal et al. (1999), Table 4 shows the SBH does not present a significant variation with the change in C_3. Additionally, little change in ESS and RAS concentration shows these two performance indicators are also insensitive to the change in C_3. However, a 20% increase in the original inflow rate (1.2Q = 1,800 m^3/hr, MLSS = 4,600 mg/L, RAS ratio = 0.8) changes the pattern for all turbulent quantities (turbulent intensity, TKE, and turbulent viscosity) from a decrease in turbulent quantities with increasing C_3 to a variable pattern, decreasing and increasing the turbulent quantities with increasing C_3. Equation 6 shows the C_μ of the Realizable k-ε model is not a constant as it in the SKE model, but a function of the mean strain and rotation rates, the angular velocity of the system rotation, and the turbulent fields. Therefore, the uncertainty of C_μ may result in unexpected changes in turbulent viscosity. Additionally, variations of SBH, ESS, and RAS concentrations as the variation of C_3 at 1.2Q are negligible. Therefore, the effects of C_3 on the SBH, ESS, and RAS concentrations at the different inflow rates are minimal.

Effects of the turbulent Schmidt number σ_c

To understand the effects of the turbulent Schmidt number on the performance of an SST, simulations are run with three turbulent Schmidt numbers (0.5, 0.7, and 1.0) at two inflow rates (Q and 1.2Q, MLSS = 4,600 mg/L, RAS ratio = 0.8) and two values of C_3. The ESS, RAS concentration, and SBH predicted at the two inflow rates and two C_3 coefficient values are shown in Figure 8a–f. They show that the ESS and RAS only change slightly with the increase in turbulent Schmidt number. This is consistent with the results in Stamou et al. (1989), who concluded that the ESS is insensitive to any change in turbulent Schmidt number. However, the variation of SBH predicted with different σ_c is significant. Figure 8e shows the SBH increases by 0.5 m (18.5%) with an increase in the turbulent Schmidt number from 0.5 to 0.7. Figure 8f shows the SBH increases by 0.6 m (24%) as the turbulent Schmidt number increases from 0.5 to 1.0. Because of space limits, the concentration profiles predicted with only two turbulent Schmidt numbers (0.5 and 1.0) at 1.2Q are presented in Figure 9a,b, to show the difference of the SBH.

Conclusions

In this study, a Fluent-based two-dimensional axisymmetric numerical model is used to study the effects of buoyancy terms in the TKE equation, and the effects of the two model parameters [the coefficient of buoyancy term (C_3) in the TDR equation and the turbulent Schmidt number (σ_c) in the sludge transport equation] on the performance of an SST. Unlike the early numerical studies that were limited by the performance of computer hardware, and convergence difficulties of SST models with high MLSS concentrations, this study provides a sensitivity analysis. The advanced SST numerical model accounts for the effects of these influential factors on the hydrodynamics and performance indicators of an SST, such as turbulent viscosity, TKE, turbulent intensity, SBH, ESS, and RAS concentrations.

Based on the simulation results, the following conclusions are made and briefly summarized in Table 5:

Table 5. Effects of each influential factor on performance indicators.

	ESS	SBH	RAS
G_b in the TKE equation	√	√	√
C_3 in the TDR equation	×	×	×
σ_c in the sludge transport equation	×	√	×

Notes. √: Strong Influence; ×: No Strong Influence.

1. The buoyancy term should be coupled in TKE to correctly predict the ESS, unless both MLSS is very low (below 1,500 mg/L) and sludge settling is high (above 13 m/hr). Field observations and results predicted by the buoyancy-coupled TKE equation at higher MLSS and poorer sludge settling show the SST is operating well; however, the buoyancy-decoupled TKE equation shows failure of the SST as a result of rising SBH, for these same conditions.
2. ESS, RAS concentrations, and SBH are all insensitive to variation of the coefficient C_3 of the buoyancy term in the TDR equation. Therefore, C_3 can be set to zero, which will remove the buoyancy term from the TDR equation, improving the rate of convergence and reducing computing time.
3. ESS and RAS concentrations are insensitive to the effects of turbulent Schmidt number σ_c, whereas SBH is strongly influenced by variation of turbulent diffusion caused by a change in σ_c. Therefore, the turbulent Schmidt number can be used to adjust the SBH, when ESS and RAS concentrations are well calibrated to the field data, but the SBH does not fit field observations.
4. It is recommended that for the application of an SST numerical model, both the prediction results of the buoyancy-decoupled and buoyancy-coupled TKE equations should be verified with the field data, before further applications of the model.

References

Adams, E. W., & Rodi, W. (1990). Modeling flow and mixing in sedimentation tanks. *Journal of Hydraulic Engineering*, *116*(7), 895–913. https://doi.org/10.1061/(ASCE)0733-9429(1990)116:7(895)

Coe, H., & Clevenger, G. H. (1916). Method for determining the capacities of slime settling tanks. *Transactions of the American Institute of Mining and Metallurgical Engineers*, *55*, 35–384.

Dahl, C. (1993). Numerical modelling of flow and settling in secondary settling tanks. Ph.D. Thesis, Aalborg University, Denmark.

Deininger, A., Günthert, F. W., & Wilderer, P. A. (1996). The influence of currents on circular secondary clarifier performance and design. *Water Science and Technology*, *34*(3–4), 405–412. https://doi.org/10.2166/wst.1996.0457

DeVantier, B. A., & Larock, B. E. (1986). Modelling a recirculating density-driven turbulent flow. *International Journal for Numerical Methods in Fluids*, *6*(4), 241–253. https://doi.org/10.1002/(ISSN)1097-0363

DeVantier, B. A., & Larock, B. E. (1987). Modeling sediment-induced density currents in sedimentation basins. *Journal of Hydraulic Engineering*, *113*(1), 80–94. https://doi.org/10.1061/(ASCE)0733-9429(1987)113:1(80)

Ekama, G. A., & Marais, P. (2002). Hydrodynamic modelling of secondary settling tanks, Part 1: Application of a hydrodynamic model to full scale secondary settling tanks. Water Research Group Report No. 835/1/02; Cape Town, South Africa: University of Cape Town.

Gao, H., & Stenstrom, M. K. (2017). Computational fluid dynamics applied to secondary clarifier analysis. In C. N. Dunn & B. VanWeele (Eds.), *World Environmental and Water Resources Congress 2017: Water, Wastewater, and Stormwater; Urban Watershed Management; and Municipal Water Infrastructure* (pp. 301–315). Sacramento, CA: ASCE. https://doi.org/10.1061/9780784480632

Gao, H., & Stenstrom, M. K. (2018). Evaluation of three turbulence models in predicting of the hydrodynamics of a secondary sedimentation tank. *Water Research*, *143*, 445–456. https://doi.org/10.1016/j.watres.2018.06.067

Griborio, A. (2004). *Secondary clarifier modeling: A multi-process approach*. Ph.D. Thesis, New Orleans University, New Orleans, Louisiana.

Hwang, H. J., & Stenstrom, M. K. (1985). Evaluation of fine-bubble alpha factors in near-full scale equipment. *Journal of WPCF*, *57*(12), 1142–1151.

Imam, E., McCorquodale, J. A., & Bewtra, J. K. (1983). Numerical modeling of sedimentation tanks. *Journal of Hydraulic Engineering*, *109*(12), 1740–1754. https://doi.org/10.1061/(ASCE)0733-9429(1983)109:12(1740)

Krebs, P., Vischer, D., & Gujer, W. (1995). Inlet-structure design for final clarifiers. *Journal of Environmental Engineering*, *121*(8), 558–564. https://doi.org/10.1061/(ASCE)0733-9372(1995)121:8(558)

Lakehal, D., Krebs, P., Krijgsman, J., & Rodi, W. (1999). Computing shear flow and sludge blanket in secondary clarifiers. *Journal of Hydraulic Engineering*, *125*(3), 253–262. https://doi.org/10.1061/(ASCE)0733-9429(1999)125:3(253)

Larsen, P. (1977). *On the hydraulics of rectangular settling basins: Experimental and theoretical studies*. Report No. 1001; Department of Water Resources and Engineering, Lund Inst. Technol., Lund University, Sweden. https://doi.org/10.1061/(ASCE)0733-9429(1994)120:2(279)

Li, B., & Stenstrom, M. K. (2014). Research advances and challenges in one-dimensional modeling of secondary settling tanks – A critical review. *Water Research*, *65*(15), 40–63. https://doi.org/10.1016/j.watres.2014.07.007

Lyn, D. A., Stamou, A. I., & Rodi, W. (1992). Density currents and shear-induced flocculation in sedimentation tanks. *Journal of Hydraulic Engineering*, *118*(6), 849–867. https://doi.org/10.1061/(ASCE)0733-9429(1992)118:6(849)

Parker, D. S. (1983). Assessment of secondary clarification design concepts. *Journal of the Water Pollution Control Federation*, *55*(4), 349–359.

Patziger, M. (2016). Computational fluid dynamics investigation of shallow circular secondary settling tanks: Inlet geometry and performance indicators. *Chemical Engineering Research and Design*, *112*, 122–131. https://doi.org/10.1016/j.cherd.2016.06.018

Ramin, E., Wágner, D. S., Yde, L., Binning, P. J., Rasmussen, M. R., Mikkelsen, P. S., & Plósz, B. G. (2014). A new settling velocity model to describe secondary sedimentation. Water Research, 66(1), 447–458. https://doi.org/10.1016/j.watres.2014.08.034

Saffarian, M. R., Hamedi, M. H., & Shams, M. (2010). Comparison of various settling velocity functions and non-newtonian fluid models in circular secondary clarifiers. Korean Journal of Chemical Engineering, *27*(5), 1497–1508. https://doi.org/10.1007/s11814-010-0253-0

Shahrokhi, M., Rostami, F., Said, M. A. M., Yazdi, S. R. S., & Syafalni (2013). Experimental investigation of the influence of baffle position on the flow field, sediment concentration, and efficiency of rectangular primary sedimentation tanks. *Journal of Hydraulic Engineering*, *139*(1), 88–94. https://doi.org/10.1061/(ASCE)HY.1943-7900.0000598

Stamou, A. I., Adams, E. W., & Rodi, W. (1989). Numerical modeling of flow and settling in primary rectangular clarifiers. *Journal of Hydraulic Research*, *27*(5), 665–682. https://doi.org/10.1080/00221688909499117

Takács, I., Patry, G. G., & Nolasco, D. (1991). A dynamic model of the clarification-thickening process. *Water Research*, *25*(10), 1263–1271. https://doi.org/10.1016/0043-1354(91)90066-Y

Tamayol, A., Firoozabadi, B., & Ashjari, M. (2009). Hydrodynamics of secondary settling tanks and increasing their performance using baffles. *Journal of Environmental Engineering*, *136*(1), 32–39.

Vitasovic, Z. C., Zhou, S., McCorquodale, J. A., & Lingren, K. (1997). Secondary clarifier analysis using data from the clarifier research technical committee protocol. *Water Environment Research*, *69*(5), 999–1007. https://doi.org/10.2175/106143097X125696

Xanthos, S., Gong, M., Ramalingam, K., Fillos, J., Deur, A., Beckmann, K., & McCorquodale, J. A. (2010). Performance assessment of secondary settling tanks using CFD modeling. Water Resources Management, *25*(4), 1169–1182.

Zhou, S., & McCorquodale, J. A. (1992a). Influence of skirt radius on performance of circular clarifier with density stratification. *International Journal for Numerical Methods in Fluids*, *14*(8), 919–934. https://doi.org/10.1002/(ISSN)1097-0363

Zhou, S., & McCorquodale, J. A. (1992b). Mathematical modelling of a circular clarifier. *Canadian Journal of Civil Engineering*, *19*(3), 365–374. https://doi.org/10.1139/l92-044

Zhou, S., & McCorquodale, J. A. (1992c). Modeling of rectangular settling tanks. *Journal of Hydraulic Engineering*, *118*(10), 1391–1405. https://doi.org/10.1061/(ASCE)0733-9429(1992)118:10(1391)

Zhou, S., & McCorquodale, J. A. (1994). Modeling of rectangular settling tanks-closure. Journal of Hydraulic Engineering, 120(2), 279–281.